

Android GNSS Measurements under Spoofing and Interference

Andrea Botticella^{*†}
andrea.botticella@studenti.polito.it

Renato Mignone^{*†}
renato.mignone@studenti.polito.it

Elia Innocenti^{*†}
elia.innocenti@studenti.polito.it

Simone Romano^{*†}
simone.romano2@studenti.polito.it

ABSTRACT

This laboratory exercise examines how consumer smartphones process raw GNSS measurements under both stationary and motion conditions, and evaluates the impact of imposed spoofed location inputs and timing delays on computed navigation solutions. Leveraging open-source filtering and weighted least-squares estimation, we measure deviations in reported fixes and identify key factors—geometry shifts, signal strength fluctuations, and clock behavior—that influence accuracy. Our findings underscore strategies for detecting anomalous GNSS outputs on mobile devices.

1 INTRODUCTION

Global Navigation Satellite Systems (GNSS) provide critical positioning services to a wide range of consumer and industrial applications. GNSS signals are however vulnerable to spoofing attacks, where artificial signal parameters are received at the receiver, which may result in false location or time estimates. It is valuable to understand the behavior of smartphone GNSS observables under legitimate and spoofed inputs to develop reliable detection methods. This lab exercise captures raw GNSS measurements from an Android smartphone under two scenarios: a rooftop static test and a kinematic trial on a tram. We run each dataset twice through a weighted least-squares estimator—once to deliver baseline performance and once with overridden reference location and controlled timing delays. In comparing the runs, we thereby isolate the effect of satellite geometry, signal quality, and receiver clock performance on output integrity. The remainder of this report is organized as follows. Section 2 describes the experimental setup, including device configuration, data collection procedures, and the processing pipeline. Section 3 presents results and discussion, contrasting static versus dynamic performance, examining spoofed-location impacts, and analyzing delay effects. Finally, Section 4 summarizes the key findings and outlines directions for future work.

2 METHODS

2.1 Devices and Software

We used a Samsung Galaxy A51 with Android 11 for this experiment. GNSS Logger v3.1.0.4 was chosen due to its unrestricted access to raw GNSS measurements, compatibility with newer Android APIs, and ability to record detailed GNSS data that is suitable for precise analysis. MATLAB R2024b was employed to handle data because it comes with Google's GNSS toolbox, which accommodates robust

analysis and visualization of GNSS measurements and position solutions.

2.2 Data Collection Procedure

Two distinct 5-minute GNSS data logging sessions were conducted on 3 May 2025, under cloudy weather conditions, using the GNSS Logger app configured with the following settings enabled:

- **GNSS Location:** Enabled to capture location data.
- **GNSS Measurements:** Enabled to log raw GNSS measurements.
- **Navigation Messages:** Enabled to capture navigation data.
- **GnssStatus:** Enabled to log GNSS status information.
- **Sensors:** Enabled to capture sensor data.

The sessions were designed to capture both static and dynamic GNSS performance, with the following details:

- **Static Scenario:** Performed on the rooftop of Monte dei Cappuccini, Turin, starting at 10:35:20. The device was stationary throughout the entire session, providing baseline measurements.
- **Dynamic Scenario:** Conducted on tram line 15 from Piazza Castello to Piazza Vittorio Veneto, starting at 10:00:21, simulating a typical urban mobility scenario.

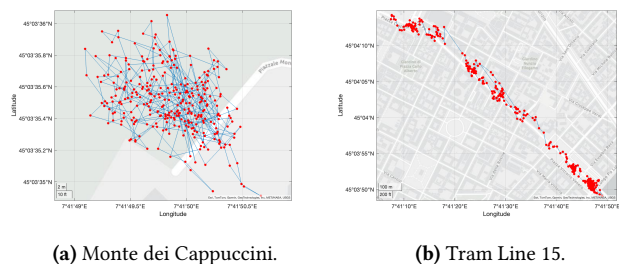


Figure 1: Comparison of GNSS data: (a) Static scenario at Monte dei Cappuccini, (b) dynamic scenario along Tram Line 15.

2.3 Processing Pipeline

The raw GNSS data from the GNSS Logger served as the input dataset for MATLAB. Processing involved a scripted workflow via `ProcessGnssMeasScript.m`, where the following steps were executed:

1. **Filtering:** Data points with a carrier-to-noise ratio below 25 dB-Hz or satellite elevations below 15° were excluded to improve accuracy.
2. **Measurement Extraction:** Pseudorange and Doppler measurements were computed from GNSS timestamps and satellite transmission data.

^{*}The authors collaborated closely in developing this project.

[†]All the authors are students at Politecnico di Torino, Turin, Italy.

59 3. **Weighted Least Squares (WLS) Positioning:** Applied to de-
60 rive precise positioning and clock bias estimates.
61 4. **Visualization and Comparison:** Output plots from MATLAB,
62 including pseudorange, pseudorange rates, and position solu-
63 tions, were generated to facilitate comparative analysis of the
64 static and dynamic scenarios.
65 Results from this processing pipeline provided insights into the
66 differences in GNSS performance under static and dynamic condi-
67 tions.

68 2.4 Spoofed-Input Configuration

69 Spoofing scenarios were emulated by introducing artificial vari-
70 ations to the recorded GNSS data through MATLAB processing.
71 Specifically, mock positions were assigned by adjusting the param-
72 eter `spoof.position`, which represents modified latitude, longi-
73 tude, and altitude coordinates. Additionally, artificial time delays
74 were tested by adjusting the `spoof.delay` parameter, typically in
75 milliseconds, to mimic delayed GNSS signal arrival. Such configu-
76 rations facilitated evaluation of the impact of spoofing scenarios
77 on position estimation reliability and accuracy.

78 2.5 Optional Interference Scenario

79 Even a worst-case interference situation was simulated, replicating
80 conditions in the vicinity of potential interference sources such
81 as broadcasting antennas or communication areas of high density.
82 GNSS data were collected near such sources of interference, and
83 then processed with the same MATLAB procedure. Nominal condi-
84 tion comparison was established to analyze the impact of external
85 interference on GNSS observables such as variation in pseudor-
86 ange measurements, carrier-to-noise ratio, and positional accuracy
87 overall.

3 RESULTS AND DISCUSSIONS

88 3.1 Baseline Performance: Static vs. Dynamic

89 3.1.1 *Static Case: Monte dei Cappuccini.* In the Monte dei Cap-
90 puccini session, the raw pseudorange measurements (Fig. ??) form
91 almost perfectly horizontal lines at around 2×10^7 m. These steady
92 tracks confirm that the receiver—and thus our antenna—remained
93 fixed on the rooftop, with only minor step-changes when the re-
94 ceiver performed clock corrections or switched satellite channels.

95 Likewise, when we compare the computed pseudorange rates
96 against the receiver’s built-in Doppler residuals (Fig. ??), the two
97 coincide to within a few centimetres per second for most satellites.
98 This near-perfect overlap tells us that, in a truly static environ-
99 ment, our Doppler estimates are highly reliable and unpolluted by
100 movement-induced biases.

101 Our C/N_0 time series (Fig. ??) shows an overall high signal
102 strength—averaging above 45 dB-Hz—but with occasional dips, for
103 example when a pylon or nearby tree briefly shadowed SV 27 around
104 50 s. Even in what we call a “static” test, local multipath can nudge
105 the carrier strength by a few dB.

106 The weighted least-squares PVT solution (Fig. ??) clusters tightly
107 around the true antenna position. The 68%-confidence horizontal
108 scatter is under 10 m, HDOP remains below 1.5, and the computed
109 speed sits at essentially zero—exactly what we expect with our

110 rooftop setup. The clock-bias drift stays under $200 \mu\text{s}$ over the entire
111 350 s run, reflecting stable timing when nothing moves.

112 Finally, the error-distribution plot (Fig. ??) offers a complete
113 picture of our static PVT accuracy. The box shows that half of all
114 horizontal errors fall between approximately 4 m and 8 m, with the
115 median line sitting right at about 6 m. The whiskers extend only as
116 far as 10 m at the upper end and 2 m at the lower end, indicating
117 very few extreme deviations. In other words, not only is our rooftop
118 setup precise on average, but even the worst-case errors remain
119 comfortably below 10 m.

120 3.1.2 *Dynamic Case: Tram Ride.* During the tram experiment,
121 the pseudorange traces (Fig. ??) still center near 2×10^7 m, but
122 we see abrupt jumps when the vehicle speeds up. For instance,
123 SV 12 exhibits a one-metre step at 120 s, coinciding with the trams
124 acceleration out of a stop.

125 The pseudorange-rate comparison (Fig. ??) now diverges from
126 the receiver’s own Doppler output by up to 0.5 m/s on some chan-
127 nels. When the tram accelerates toward SV 18, the Doppler residuals
128 dip negative—exactly as physics predicts—and match GPS velocity
129 readings that peak at around 20 m/s (72 km/h), in line with the
130 tram’s timetable.

131 Carrier-to-noise measurements (Fig. ??) reveal more volatility:
132 C/N_0 often plunges below 30 dB-Hz. These deep fades correlate
133 with our onboard camera’s view of narrow streets, underlining how
134 urban multipath and NLOS conditions degrade signal quality in
135 real transport scenarios.

136 Despite these challenges, the WLS PVT solution (Fig. ??) tracks
137 the tram’s path reasonably well. Our 68% horizontal error circle
138 expands to about 30 m, and HDOP jumps up to 5 when only 5-6
139 satellites are in view. Yet the computed speed profile still mirrors
140 the tram’s acceleration and braking phases, confirming that even
141 with urban impairments, our solver captures the true dynamics of
142 a moving vehicle.

143 The corresponding error-distribution plot for the tram ride (Fig. ??)
144 reveals a markedly wider spread. Here, the median horizontal error
145 rises to about 25 m, reflecting the challenges of urban multipath
146 and partial NLOS conditions. The interquartile box stretches from
147 roughly 15 m up to 35 m, showing that typical errors sit within
148 this band. Meanwhile, the whiskers reach out to nearly 50 m dur-
149 ing deep signal fades—such as when passing between tall build-
150 ings—and drop down to about 5 m in more open sections. This
151 narrative illustrates both the typical accuracy we can expect on a
152 moving tram and the occasional outliers that urban environments
153 introduce.

154 3.2 Impact of Spoofed Position

155 3.3 Effects of Timing Delays

156 3.4 Interference Effects

4 CONCLUSIONS

A APPENDIX

157 "Lorem ipsum dolor sit amet, consectetur adipiscing elit, sed do
158 eiusmod tempor incididunt ut labore et dolore magna aliqua. Ut
159 enim ad minim veniam, quis nostrud exercitation ullamco laboris
160 nisi ut aliquip ex ea commodo consequat. Duis aute irure dolor in
161 reprehenderit in voluptate velit esse cillum dolore eu fugiat nulla
162 pariatur. Excepteur sint occaecat cupidatat non proident, sunt in
163 culpa qui officia deserunt mollit anim id est laborum."